Organization and Dynamics of the Proteolipid Complexes Formed by Annexin V and Lipids in Planar Supported Lipid Bilayers

Laurence Cézanne,* André Lopez, Florence Loste, Géraldine Parnaud, Olivier Saurel, Pascal Demange, and Jean-François Tocanne

Institut de Pharmacologie et de Biologie Structurale du CNRS, 118, Route de Narbonne, F-31062 Toulouse Cedex, France

Received August 3, 1998; Revised Manuscript Received November 9, 1998

ABSTRACT: The consequences of the binding of annexin V on its lateral mobility and that of lipids were investigated by means of experimental and simulated FRAP experiments. Experiments were carried out on planar supported bilayers (PC/PS 9:1 mol/mol mixtures) in the presence of 1 mM $CaCl_2$ in the subphase. The probes C_{12}-NBD-PS and fluorescein-labeled annexin V were used and the data compared with that previously obtained for C_{12}-NBD-PC [Saurel, O., Cézanne, L., Milon, A., Tocanne, J. F., & Demange, P. (1998) *Biochemistry 37,* 1403−1410]. At complete coverage of the lipid bilayer by the protein ($C_{annexin}$ = 80 nM), the lateral mobility of C_{12}-NBD-PC was reduced by 40% while C_{12}-NBD-PS and bound annexin V molecules were nearly immobilized ($D < 10^{-11}$ cm^2/s). At moderate protein concentration (20 nM < $C_{annexin}$ < 80 nM), best fitting of the lipid and protein probe recoveries was achieved with one single diffusion coefficient and a mobile fraction close to 100%, indicating homogeneous lipid and protein populations. In contrast, at low protein concentration ($C_{annexin}$ < 20 nM), C_{12}-NBD-PS showed a two-component diffusion. The slow PS population at $C_{annexin}$ < 20 nM and the single PS population at $C_{annexin}$ > 20 nM moved at the same rate that bound annexin V (mobile fraction close to 100%), indicating strong PS/protein interactions. With the aid of computer simulations of the lateral motion of PC molecules, based on the 2-D crystalline networks formed by annexin V in contact with the lipid bilayer, these FRAP results may be accounted for by considering a rather simple model of a proteolipidic complex consisting of an extended 2-D crystalline protein network facing the lipid bilayer and stabilized by strong interactions between annexin V and PS molecules. In this model, immobilization of annexin V and PS molecules originates from their mutual interactions. The slowing down of PC molecules is due to various obstacles to their lateral diffusion which can be described as: the four PS molecules bound to the protein, the tryptophan 187 which presumably interacts with the lipids at the level of their polar headgroups and probably the three other hydrophobic amino acid residues located on the AB calcium-binding loops of the protein.

Annexins constitute a large family of structurally related proteins which share the common characteristic of binding strongly to phospholipids in a calcium-dependent manner (*1, 2*). These proteins are widely spread in many eukaryotic organisms. Today, 13 different annexin subclasses are recognized which all exhibit, in their amino acid sequences, a central core composed of four highly conserved domains (*3*). Although various potential activities have been inferred from in vitro investigations (blood coagulation, signal transduction, anti-inflammatory processes, membrane trafficking, and ion channel activity), the real biological functions of annexins remain to be elucidated (for recent reviews, see refs *4* and *5*). The structure of some of the members of the family, especially annexin V, has been elucidated at the atomic level. Structural data have been obtained from X-ray diffraction studies on 3-D[1] protein crystals (*6*−*10*) and at lower resolution from electron microscopy studies on 2-D protein crystals formed in contact with lipid monolayers (*11, 12*). In contrast, the structure of the proteolipid complexes formed when annexins interact with lipids is still unknown. In particular, the influence of these proteins on the organization and dynamics of lipids remains poorly documented. However, this point is of particular interest because the biological functions of annexins are believed to depend primarily on their interactions with lipids in membranes. In this respect, and in connection with the calcium channel activity demonstrated for annexin V in membrane model systems (*13*), we recently asked the question of whether this protein can alter the "fluidity" of membrane lipids, the term fluidity being understood in its largest meaning, including the conformational, rotational, and translational mobilities of lipids (*14*). These parameters were studied using ^{2}H and ^{31}P NMR spectroscopy, fluorescence polarization, and fluo-

* To whom all correspondence should be adressed.

[1] Abbreviations: PC, phosphatidylcholine; PS, phosphatidylserine; C_{12}-NBD-PC, 1-acyl-2[12-[(7-nitro-2-1,3-benzoxadiazol-4-yl)amino]-dodecanoyl]-phosphatidylcholine; C_{12}-NBD-PS, 1-oleoyl-2-[12-[(7-nitro-2-1,3-benzoxadiazol-4-yl)amino]dodecanoyl]-phospho-L-serine; FRAP, fluorescence recovery after photobleaching; NMR, nuclear magnetic resonance; AFM, atomic force microscopy; 2-D, bi-dimensional; 3-D, tri-dimensional; FITC, fluorescein isothiocyanate; HEPES, 4-(2-hydroxyethyl)-1-piperazineethanesulfonic acid; EDTA, ethylenediaminetetraacetic acid; SDS−PAGE, sodium dodecyl sulfate−polyacrylamide gel electrophoresis.

10.1021/bi9818568 CCC: $18.00
Published on Web 02/10/1999

rescence recovery after photobleaching (FRAP) experiments carried out on lipid vesicles and planar supported lipid bilayers composed of phosphatidylcholine/phosphatidylserine mixtures (*14*). The main result of this investigation was that annexin V, even at complete coverage of the lipid bilayers, showed no influence on the lipid molecular packing and the acyl chain flexibility of both PC and PS molecules. In contrast, the protein strongly affected the lateral motion of the lipids, with a marked reduction of the diffusion rate of PC and a nearby immobilization of PS. From these results, it was suggested that annexin V entered a proteolipid complex in the form of an extended 2-D network in contact with the lipid bilayer, stabilized by strong interactions with PS molecules (*14*).

To go further in the elucidation of the organization of this proteolipid complex, we undertook a detailed study of the lateral motions of PS and annexin V molecules using FRAP experiments. This study was carried out with planar supported lipid bilayers composed of lipids in the liquid crystalline state with specifically NBD-labeled PS probes and with fluorescein-labeled annexin V molecules. The FRAP data so obtained and the previous results related to PC molecules (*14*) were then combined with computer simulations of the diffusional behavior of the lipids for various structural models of the proteolipid complex based on the various 2-D networks which have been put forward for annexin V in contact with lipid layers by electron microscopy (*11, 12*) and atomic force microscopy (*15*).

MATERIALS AND METHODS

Chemicals. Egg yolk L-α-phosphatidylcholine (egg-PC) and bovine brain L-α-phosphatidyl-L-serine (brain-PS), FITC isomer I, and glycine were purchased from Sigma Chemical Co. (St Louis, MO). 1-Oleoyl-2-[12-[(7-nitro-2-1,3-benzoxadiazol-4-yl)amino]dodecanoyl]-phospho-L-serine (C_{12}-NBD-PS) was purchased from Avanti Polar Lipids (Birmingham, AL). Phospholipids and the fluorescent probe were pure as checked by thin-layer chromatography. They were used without further purification. Salts and solvents were of analytical grade. The concentration of phospholipids in stock solutions was determined by phosphorus assay (*16*).

Expression of Annexin V in Escherichia coli. Annexin V was expressed in BL21DE3 *E. coli* strain electrotransformed with pRSET AV vector as described elsewhere (*17*). The purification of the human recombinant protein relied on its calcium-dependent binding to bovine brain lipids (*18*). The purity of annexin V was controlled by 15% SDS−PAGE (blue coomassie staining) and electrospray mass spectrometry (*17*). The concentration of annexin V in stock solutions was determined by absorption spectroscopy using a molar extinction coefficient of 22 000 M^{-1}/cm at 280 nm (*19*).

Labeling of Annexin V with Fluorescein. Purified annexin V was dialyzed against the labeling buffer (150 mM NaCl, 1 mM $CaCl_2$, 10 mM sodium borate, pH 9.0). Annexin V (50 μmol) was added to FITC isomer I (1 mmol), and the mixture was kept 16 h at 4 °C in the dark. The reaction was stopped by the addition of glycine (10 mmol). The fluorescent protein was purified by gel filtration on a PD 10 column (Pharmacia Biotechnology). Its purity was checked by 15% SDS−PAGE experiment and electrospray mass spectrometry. Under the experimental conditions used, labeling of annexin V was limited to ∼1 FITC per protein molecule.

Preparation of Planar Supported Lipid Bilayers. Planar supported lipid bilayers were formed by adsorption and fusion of Small Unilamellar Vesicles (SUV) on cleaned glass coverslips mounted on a small Plexiglas tank adapted to the microscope stage (*14, 20*−*23*). SUVs were prepared with egg-PC/brain-PS (9:1 mol/mol) labeled with 1 mol % C_{12}-NBD-PS. The desired amounts of phosphatidylcholine, phosphatidylserine, and lipid probe were taken from stock solutions in chloroform and mixed together. The mixture was dried under nitrogen at 40 °C, and traces of solvent were removed under vacuum. Lipids (2 mg) were suspended in 1 mL of the suspension buffer A (10 mM Na_2HPO_4, 100 mM NaCl, pH 7.2). The lipid suspension was sonicated for 15 min in pulsed mode at 30 mW (50% duty cycle) using a tip Branson B15 sonifier. Titanium particles were eliminated by centrifugation (13400*g*, 10 min) using a bench centrifuge. Cleaning of the coverslip was of prime importance with respect to the formation of the bilayer. Coverslips were first rinsed with ethanol 95%, washed with deionized water (MilliQ plus 185, Millipore) then immersed for 30 min in sulfochromic acid, and finally washed extensively (15 times) in large volumes of deionized water. To protect them from dust or contamination, we stored the clean coverslips in deionized water. Just before use, one coverslip was taken out of water and placed on the top of the sample cell. The cell was filled with the SUV suspension (diluted to a concentration of 0.2 mg/mL in the same buffer A) up to contact with the coverslip. Spontaneous adsorption and fusion of vesicles on the glass surface led to the formation of a stable planar supported lipid bilayer (*14, 20*−*23*). After 2 h of incubation and to avoid any problem due to the formation of complexes between the phosphate anions and the calcium ions which are required for the binding of annexin V to the acidic phospholipids, we exchanged phosphate buffer A in the cell slowly with 1 volume of the assay buffer B (10 mM HEPES, 100 mM NaCl, pH 7.4). Calcium ions were added in the subphase at the final concentration of 1 mM. Then annexin V was added to the subphase at various concentrations. At the end of a set of FRAP experiments, EDTA (5 mM) was added to the subphase to check the reversibility of the binding of annexin V to the lipid bilayer. After each addition of calcium ions, annexin V, or EDTA, the cell was equilibrated for 30 min at 20 °C before starting FRAP experiments.

FRAP Experiments. Experiments were carried out under conditions of constant incident light intensity and of "uniform disk illumination", using an apparatus based on a Leitz Ortholux II fluorescence microscope (*24*). The excitation beam from a mercury arc lamp was focused on samples through a Leitz x63/1.3 oil immersion objective. The radius of the illuminated area was 2.95 μm. For both the NBD-labeled PS and the FITC-labeled protein, bleaching rates of around 40% were obtained for a bleaching time of 250 ms. This bleaching time was consistent with the 2 s recovery half-time currently found for lipids in planar supported lipid bilayers. At least 40 fluorescence recoveries were accumulated for each experimental condition tested. All experiments were carried out in triplicate.

Computer-Simulated FRAP Experiments. The computer generation of simulated FRAP experiments has already been described in detail (*25, 26*). In this report, we will just consider the features which are important with respect to

the specific case we studied. The membrane is represented by a 150 × 150 site triangular lattice. Each site can be empty or bear an immobile obstacle or a mobile point which represents a diffusing particle. In the following, these mobile points will be referred to as the tracers. Lateral diffusion of tracers is followed by sequential reading of all of the matrix sites. One reading of the matrix defines a time-step, the time unit of the system. When a tracer is found on a site, a jump direction from this site to one of the six closest neighbors is chosen at random. Because tracers are considered to be independent of each other, two tracers or more are allowed to occupy the same site. Therefore, if the site chosen for the jump is free or occupied by a tracer, the jump can occur. If the site under consideration bears more than one tracer, the process is repeated until all tracers are examined. If the site chosen is occupied by an obstacle, then the jump is not allowed and the tracer stays in its initial site until the next time-step. Thus a time-step corresponds to a jump (or a jump attempt) for all of the tracers present in the matrix. Due to the finite size of the matrix, periodic boundary conditions were used.

To generate a recovery curve, we first introduced point obstacles at a given surface density and distributed them spatially in the matrix. The obstacle surface density and spatial distribution were both imposed by the type of 2-D network chosen for the annexin V molecules in contact with the lipid bilayer (see Discussion and Figure 4). The position of this obstacle network in the matrix was defined at random and therefore changed from one recovery curve to the other. Then, 2000 point tracers were distributed randomly in the matrix, on the obstacle-free sites. These tracers are equivalent to the lipid probes used in the real FRAP experiments. To simulate FRAP experiments, a circular area of observation of radius $R = 20$ lattice spacings (ls) was introduced at the center of the matrix. The initial fluorescence intensity I_o was determined by computing the average number of tracers present inside the observation area over 100 time-steps. To simulate the bleaching step, we suppressed all of the tracers present in the observation area. For the recovery step, the fluorescence intensity I(t) was evaluated at each time-step by calculating the number of tracers which had returned to the observation area and that over a sufficient number of time-steps for complete re-equilibration of tracers between the bleached and nonbleached areas to be reached. Typically, 1500 time-steps were needed for a complete recovery of the tracers to be observed. Each distinct simulated recovery obtained in this way exhibited the typical shape of an experimental recovery curve. However, due to the finite size of the matrix and the limited number of tracers therefore observed, these recoveries were noisy and were affected by the relative position of the observation area and obstacle network. Consequently, at least 250 distinct recoveries were computed and averaged. The decision to stop accumulation was made after checking that further accumulation of recoveries did not modify the final diffusion coefficient D and the mobile fraction M solution values.

For both the simulated and experimental FRAP data, we will consider the relative diffusion coefficient D^* calculated as the ratio $D^* = D/D_0$ of the diffusion coefficients measured, respectively, in the presence (D) and in the absence (D_0) of obstacles in the lipid matrix.

Analysis of FRAP Data. The diffusion coefficient D and the mobile fraction M were obtained by fitting classical equations of diffusion to the experimental and simulated recovery curves, as already described (*24*). A minimization algorithm coupled to statistical analysis of the data was used which, from a set of accumulated recovery curves, provides the solution value for D and M and their maximum (D_{max}, M_{max}) and minimum (D_{min}, M_{min}) values for a certain degree of confidence (*24*). In addition to and using the criterium of minimum square deviation, it was possible to achieve the best fitting of the experimental recovery curves with one or two diffusion coefficients. In the present work, D and M are given at a 95% confidence level. From a strictly statistical point of view, D values can be considered to be different from each other only in the absence of overlap between the extreme D_{min} and D_{max} values.

RESULTS

(1) Preliminary Remarks. As in our previous work (*14*), the composition of the lipid bilayer was 90 mol % egg-PC for 10 mol % brain-PS. The presence of phosphatidylserine is essential for the binding of annexin V to the lipid bilayer. Assuming that in a 2-D network of annexin V at the bilayer surface one molecule of protein occupies on average an area of 31 nm^2 (*12*), and taking a molecular area of 0.63 nm^2 for the lipids in the fluid phase (*27*), one annexin V is associated on average with about 50 lipids (*14*). In the case of complete covering of the bilayer surface by the protein, this means that 5 PS molecules are available on average per annexin V molecule, a ratio close to the stoichiometric ratio of four phosphatidylserine molecules per protein molecule (*6*).

The following important points should be recalled. (i) Planar supported lipid bilayers were formed in contact with cleaned glass coverslips by adsorption and fusion of small unilamellar lipid vesicles (*14*, *20*−*23*). This well-characterized procedure led to the formation of a single lipid bilayer (*14*). (ii) The binding of annexin V to lipid bilayers was monitored using FITC-labeled annexin V and in the absence of NBD-labeled phospholipids in the lipid bilayer (*14*). As recalled in Figure 1, the fluorescence signal, IF, detected by the FRAP apparatus at the level of the lipid bilayer, rapidly increased upon addition of annexin V in the subphase and saturation was reached for a protein concentration of 80 nM. Binding of the protein occurred without penetration into the lipid bilayer and was shown to be reversible after the addition of EDTA in the subphase (*14*).

(2) Influence of Annexin V on the Lateral Diffusion of Lipids. FRAP experiments were carried out after 30 min of incubation of the protein with the lipid bilayer. This was the time required for protein/lipid interactions to reach equilibrium and for the bilayer to stabilize as was inferred from the great stability of the fluorescence signal (*14*). In what follows and to account for possible fluctuations in D from one bilayer to the other, we will consider the relative diffusion coefficient D^* calculated as the ratio $D^* = D/D_0$ of the diffusion coefficients measured, respectively, in the presence (D) and in the absence (D_0) of annexin V for a given bilayer.

(a) Influence of Annexin V on the Lateral Diffusion of the Probe C_{12}-NBD-PC. As previously reported (*14*) and as recalled in Figure 1, D^* rapidly decreased down to 0.64 for

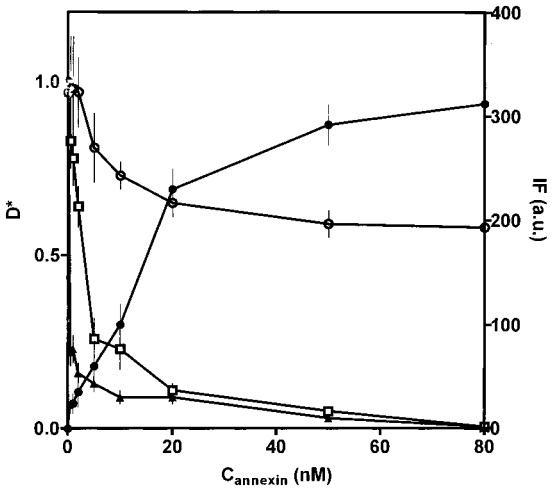

FIGURE 1: Influence of annexin V concentration on the lateral motion of the probes C_{12}-NBD-PC (○) and C_{12}-NBD-PS (▲, □) in egg-PC/brain-PS (9:1, mol/mol) planar supported bilayers. Results are provided in terms of the relative diffusion coefficient $D^* = D/D_0$. D and D_0 are the diffusion coefficients measured in the presence and absence of protein, respectively. For C_{12}-NBD-PC (○), the best fitting of the fluorescence recovery curves was achieved with a single diffusion coefficient. For C_{12}-NBD-PS, two coefficients were required, indicating the presence of slowly diffusing (▲) and rapidly (□) diffusing PS species within the same bilayer. Also shown is the binding curve of FITC-labeled annexin V molecules to the lipid bilayer (●). The data (○ and ●) was taken from Saurel et al. (*14*). $CaCl_2$ concentration in the subphase was 1 mM and temperature was 20 °C.

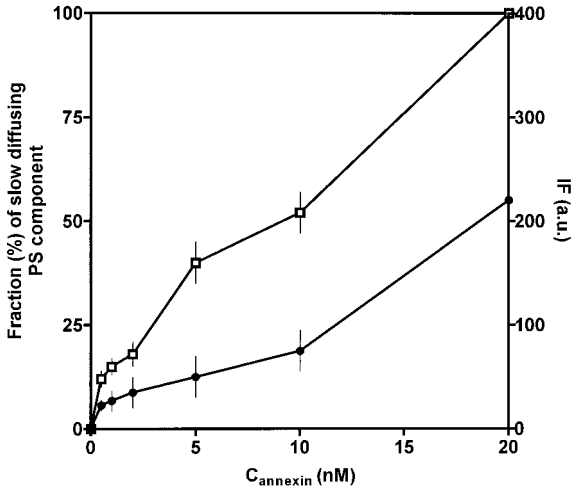

FIGURE 2: Influence of annexin V concentration on the binding of FITC-labeled annexin V molecules to the lipid planar supported bilayer (●) and on the fraction of slowly diffusing phosphatidylserine molecules (□).

a protein concentration $C_{annexin}$ of 20 nM and then stabilized around a value of 0.6 for a $C_{annexin}$ of 80 nM. The recovery curves were reanalyzed, and as a new result, it is worth noting that at any protein concentration the best fitting of these curves to the equations of diffusion was achieved with a single diffusion coefficient only. The mobile fraction M remained unchanged, close to 100%.

(b) Influence of Annexin V on the Lateral Diffusion of the Probe C_{12}-NBD-PS. In the absence of annexin V, the best fitting of the C_{12}-NBD-PS recovery curves was achieved with a single diffusion coefficient of $1 \pm 0.07\ 10^{-8}$ cm^2/s, close to that of $0.8 \pm 0.05\ 10^{-8}$ cm^2/s found for C_{12}-NBD-PC under the same experimental conditions. In the experiments described below, binding of annexin V to the lipid bilayer was achieved in the presence of 1 mM $CaCl_2$ in the subphase. At this concentration and as previously found for the probe C_{12}-NBD-PC (*14*), calcium ions had no influence on the lateral motion of C_{12}-NBD-PS.

Upon addition of annexin V in the subphase, C_{12}-NBD-PS was much more affected in its lateral motion and in a more complex manner than C_{12}-NBD-PC. Thus, a 90% reduction in D was already observed for the moderate protein concentration of 20 nM. At saturation ($C_{annexin} = 80$ nM), the probe stopped moving laterally, at least over the time span of our FRAP experiments (∼10 min), as attested by the absence of any measurable fluorescence recovery. Still on the basis of the best fitting of the recovery data, the single diffusion coefficient observed in the absence of annexin V split into two diffusion coefficients for $C_{annexin} < 20$ nM, while a single diffusion coefficient was again sufficient for higher protein concentrations ($C_{annexin} > 20$ nM) (Figure 1). These results clearly indicate that, at low concentrations of annexin V in the subphase ($C_{annexin} < 20$ nM), two phosphatidylserine populations were coexisting within the bilayer, one diffusing rapidly and the other diffusing slowly. These diffusion coefficients were associated with mobile fractions close to 100%. As shown in Figure 2, the relative weight of the slow PS population was found to increase with annexin V concentration, in a way closely related to the binding of the protein to the lipid bilayer.

It was important to check that the immobilization of C_{12}-NBD-PS at saturation ($C_{annexin} = 80$ nM) was not an artifact due to an alteration of the physical integrity of the bilayer. At the end of a given set of FRAP experiments, EDTA was added in the subphase and D was measured again. Addition of the calcium chelating agent restored a single diffusion coefficient for the probe, close to that measured initially in the absence of annexin V ($D^* \sim 0.95-1$). This result confirmed the reversibility of the binding process and showed that the protein did not affect the structure of the lipid bilayer. The same conclusion was reached with the probe C_{12}-NBD-PC (*14*).

(3) Lateral Diffusion of Annexin V in Contact to Planar Supported Lipid Bilayers. Having established that annexin V strongly affected (and in quite different ways) the lateral motion of phosphatidylcholine and phosphatidylserine molecules, it was important to examine the motional behavior of the protein itself, when adsorbed to the lipid bilayer. FITC-labeled annexin V was used, and FRAP experiments were carried out at the level of the lipid bilayer with varying the concentration of the fluorescent protein in the subphase. Results are shown in Figure 3. For $C_{annexin} = 0.5$ nM (the lowest protein concentration enabling a significant fluorescence signal to be detected at the level of the lipid bilayer, see Figure 1), adsorbed protein molecules showed a D value of $0.55 \pm 0.08\ 10^{-8}$ cm^2/s. Upon increasing the protein subphase concentration, the diffusion coefficient of the adsorbed protein molecules dropped sharply (D values of $0.2\ 10^{-8}$ and $0.1\ 10^{-8}$ cm^2/s for $C_{annexin}$ of 1 and 10 nM, respectively) (Figure 3). At saturation ($C_{annexin} = 80$ nM), adsorbed annexin V molecules were found to remain immobile (absence of any measurable fluorescence recovery) within the time span of our FRAP experiments (10 min). The recovery curves obtained at low and moderate

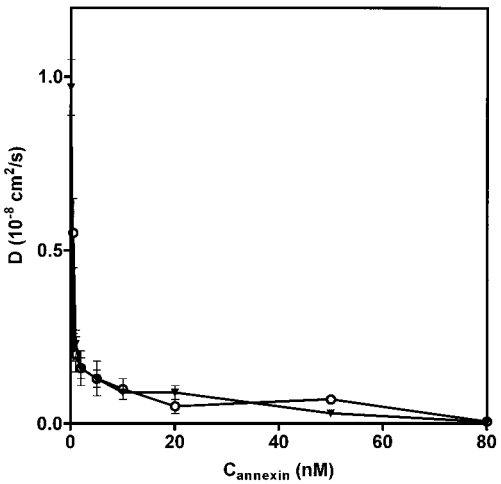

FIGURE 3: Lateral diffusion coefficient of FITC-labeled annexin V molecules bound to egg-PC/brain-PS (9:1, mol/mol) planar supported bilayers versus the protein concentration in the subphase (○). Also shown are the diffusion coefficients corresponding to the slowly diffusing C_{12}-NBD-PS species (▼). $CaCl_2$ concentration in the subphase was 1 mM and temperature was 20 °C.

protein concentrations were satisfactorily accounted for with a single diffusion coefficient and a mobile fraction close to 95−100%. Figure 3 also shows that, within experimental error, the diffusion coefficients measured for the adsorbed protein molecules and the slow PS population were the same.

(4) Computer-Simulated Lateral Diffusion of Phosphatidylcholine Molecules in the Proteolipid Complex. Results of simulation are presented in Table 1. They will be introduced in detail and analyzed in the Discussion.

DISCUSSION

In our previous communication, it was shown that annexin V strongly interacts with lipid bilayers without insertion between the lipid molecules and without significantly affecting their molecular packing (*14*). From the above, it is clear that binding of the protein to the lipids strongly affects their lateral motion but in quite different ways. Thus, great differences are observed between the C_{12}-NBD-PC and the C_{12}-NBD-PS probes, the former being slowed by 40% upon saturation and the latter being practically immobilized. These FRAP results differ from those reported for annexin IV interacting with planar supported bilayers composed of POPC/POPG mixtures (*30*). The lateral motion of these lipids was also affected by the protein, but the two probes used, NBD-PC and NBD-PG, exhibited similar diffusional behavior. Both were characterized by a two-component lateral diffusion. Decreases in *D* were related to the amount of POPG in the mixed bilayers and were significant only for relatively high protein concentrations in the subphase ($C_{annexin}$ > 80 nM). It was concluded that annexin IV induced a fluid−fluid phase separation in these bilayers in POPG-dependent fashion rather than forming long-lived stoichiometric complexes with the POPG molecules (*30*). Calcium ions might trigger lateral phase separation in PC/PS mixtures depending on their concentration in the water phase and the nature and length of the lipid acyl chains (*29, 31*). We in fact checked that, under our experimental conditions, these ions had no influence on the diffusion rate of these lipids (*14*). Furthermore, experiments carried out with pyrene-labeled phosphatidylcholine/phosphatidylserine mixtures showed that annexin V may affect the lateral motion of these lipids without inducing lateral phase separation (*32*).

Our FRAP data can be accounted for by considering a rather simple model of a proteolipidic complex consisting of an extended 2-D crystalline protein network facing the lipid bilayer and stabilized by strong interactions between annexin V and phosphatidylserine molecules. The possibility for annexin V to form 2-D crystals at water/lipid interfaces is well-documented (*11, 12, 33*). On lipid monolayers at the air/water interface, crystals with p6 (*12*) or p3 (*11*) symmetry have been detected by electron microscopy at 2 and 0.8 nm resolution. On planar supported lipid bilayers, crystals with p6 symmetry, similar to those described by Voges et al. (*12*), have been identified recently by atomic force microscopy at 2 nm resolution (*15*). In these various types of 2-D crystals, the protein lies flat on the surface of the lipid films without penetrating them. At a submolecular level, 2-D crystallization of annexin V has been shown to occur with only slight conformational changes as compared to the structure of the protein in its 3-D crystal (*12, 15*). A calcium-binding site in domain III is revealed while at the same time tryptophan 187 is exposed outwardly and has been suggested to interact with the phospholipids at least at the level of the polar headgroups (*34*−*36*).

Strong binding of PS to annexin V may be inferred from that work with the observation that (i) bound protein and slow PS molecules exhibit the same D and (ii) the weight of the slow PS component varies according to the extent of protein binding to the lipid bilayer. In the same respect, a comparative study of the crystal structure of glycerophosphoserine (GPS) or glycerophosphoethanolamine (GPE) complexes with annexin V showed specific interactions between the protein and the serine headgroup at the atomic level (*37*). This led to the conclusion that structural complementarity between the protein and the lipid headgroup may be more important than net phospholipid charge in determining selectivity (*37*). It has been suggested that bound and unbound PS molecules exchange rapidly (*38*). Actually, the fact that PS molecules such as annexin V molecules are nearly immobilized at saturation ($D < 10^{-11}$ cm^2/s) suggests the existence of a long-lived annexin V/PS complex whose lifetime (calculated from *D*, as the time required for one PS molecule to jump from one position to the next one) would be in the millisecond range or even larger.

It should also be noted that, in conditions of incomplete protein coverage, annexin V trimers as well as microcrystals were observed on lipid monolayers (*12*). At the contact of planar supported lipid bilayers, only circular crystalline domains with p6 symmetry were detected by AFM, which progressively grew with time up to coalesce (*15*). Because the AFM and the present FRAP studies were carried out under similar conditions of the membrane model system, lipid composition, calcium ions, and annexin V concentrations, it can reasonably be assumed that annexin V p6 2-D crystals also formed at the contact of our lipid bilayers.

Finally, and as was mentioned in the preliminary remarks, many control experiments showed that annexin V has access to the distal leaflet of the planar supported lipid bilayers only. This means that differences in lipid lateral mobility between the two leaflets due to interactions of the protein with only one leaflet would normally result in a two-component lateral

Table 1: Computer-Calculated Relative Diffusion Coefficients *D*c* of Lipid Molecules within a Lipid Layer for Various Types of Obstacle Distributions and Area Fractions[a]

obstacle network	obstacle nature		obstacle area fraction	relative diffusion coefficients	
annexin 2-D crystals	4PS, Trp187	4PS, Trp187, Leu31, Ala103, Ala262	*S* (%)	*D*c*	*D*r*
p6 without central trimer	+		7	0.79 ± 0.02	0.89 ± 0.02
p6 with central trimer	+		10.2	0.74 ± 0.02	0.84 ± 0.01
p6 without central trimer		+	11.1	0.68 ± 0.02	0.81 ± 0.01
p6 with central trimer		+	16.3	0.61 ± 0.02	0.74 ± 0.01
p3	+		18.2	0.61 ± 0.01	0.71 ± 0.01
p3		+	29.7	0.40 ± 0.01	0.53 ± 0.01

[a] These distributions were imposed by the structure of the annexin V crystals, with p6 or p3 symmetry (see Figure 4). The four PS molecules linked to the protein via a calcium bridge and the Trp187 residue which interacts with the lipid polar headgroups were considered as obstacles. In addition, the three hydrophobic amino acid residues Leu31, Ala103, and Ala262 which are located on the calcium-binding loops in domains I, II, and IV in close proximity to the PS-binding sites and which are liable to interact with the lipid headgroups were also considered. Also shown are the relative diffusion coefficients *D*r* calculated in each case for the same area fraction of randomly distributed obstacles.

diffusion for the lipid probes. In fact, most of the above FRAP data can be fitted with a single diffusion component. As a possible explanation, it should be observed that, in the presence of the protein, the lipid bilayer is sandwiched between two rigid supports, one provided by the glass surface and the other by the crystalline annexin V monolayer. Such a constraint may trigger a coupling between the two leaflets, as described for planar supported lipid bilayers in a liquid/solid coexistence state (*39*). This would erase differences in lipid lateral mobility between the two leaflets and thus lead to the detection of a single diffusion component for the lipids, in particular at saturation.

With this in mind the FRAP data can be accounted for in the following way. At low protein concentration in the subphase (1−2 nM), annexin V trimers may already exist at the surface of the bilayer which rapidly diffuse laterally to form small crystalline domains with symmetry p6. Consistently, a single *D* value was observed at any protein concentration, accounting for the lateral motion of protein crystals of a certain size. Upon increasing the protein concentration, the 2-D crystals grow in size and consequently the diffusion coefficient of the protein decreases. At the same time the fraction of PS molecules firmly bound to annexin V (the slow component fraction) moves like the crystals and therefore shows a diffusion coefficient similar to that measured for the protein at the same concentration. The fast PS component may correspond to those PS molecules which are still not bound to the protein crystals. For annexin V concentrations higher than 20 nM, protein coverage is near saturation. The crystalline protein domains start to coalesce, and the lateral motion of the protein is considerably reduced. Near and at saturation, practically all of the PS molecules present in the lipid film are recruited to achieve the stoichiometry of four PS molecules per annexin V molecule (remember that the lipids are composed of 10% PS and that one protein molecule is facing, on average, 50 lipid molecules). Consequently, the two *D* components found for NBD-PS fuse and the probe shows a single diffusion coefficient again whose value is similar to that measured for the protein.

At this stage, the diffusional behavior of the phosphatidylcholine molecules remains to be explained. Under the experimental conditions used this lipid does not interact with the protein (data not shown). However, the diffusion rate of NBD-PC decreased with increasing protein concentration and was reduced by 40% at saturation. At any protein concentration, the probe showed a single diffusion coefficient indicating a homogeneous PC population. These results may be explained by assuming that PS molecules, which are immobilized because of their interactions with annexin V, as well as tryptophan 187, which presumably interacts with the lipid bilayer (*34*−*36*), act as numerous immobile obstacles to the lateral motion of PC molecules. Note that Trp187 does not have to penetrate the bilayer deeply to act as an obstacle. Interactions with the lipid polar headgroups are enough. This obstacle is equivalent to a small asperity capable of preventing flat objects from sliding on a flat surface. To support this model, we carried out computer simulations of FRAP experiments using the approach which we developed for studying the influence of obstacles of various sizes and surface concentrations on the lateral diffusion of lipids in membranes (*25, 26*). Annexin V is known to strongly bind four PS molecules via the AB Ca^{2+}-binding loops in domains I (Gly30-Leu31-Gly32), II (Gly102-Ala103-Gly104), and IV (Gly261-Ala262-Gly263) and one located near Trp187 in domain III (Gly183-Glu184-Leu185-Lys186-Trp187-Gly188) (*9, 10, 40*). This means that each protein molecule can provide at least five obstacles (four PS molecules and the inserted Trp187) whose sizes are similar to that of the diffusing species, that is, a lipid molecule. Therefore, simulations were performed with point obstacles. They were distributed in the lipid matrix by reference to the 2-D crystalline networks found for the protein in contact with lipid monolayers or bilayers. The data for crystals with symmetry p6 was taken from Voges et al. (*12*) and with symmetry p3 from Brisson et al. (*11*). Figure 4 shows the spatial distribution of the PS and Trp obstacles obtained after adaptating the p6 and p3 protein crystal unit cells on the lipid matrix, using a molecular area of 0.63 nm^2 for the lipids in the liquid phase (*27*). It should be stressed that, in the p6 crystal, six annexin V trimers are arranged in the form of a crown with symmetry p6, while a seventh trimer is located, in a noncrystallographic manner, at the 6-fold symmetry center (*12, 15*). Depending on the protein concentration this central trimer may be absent or present (*15*). When present this trimer was assumed fixed, its orientation was taken as that of one of the trimers in the crown by simple homothetic translation. Finally, the relative diffusion coefficient *D*c* values calculated for a given obstacle configuration were systematically compared to *D*r* values obtained for the same

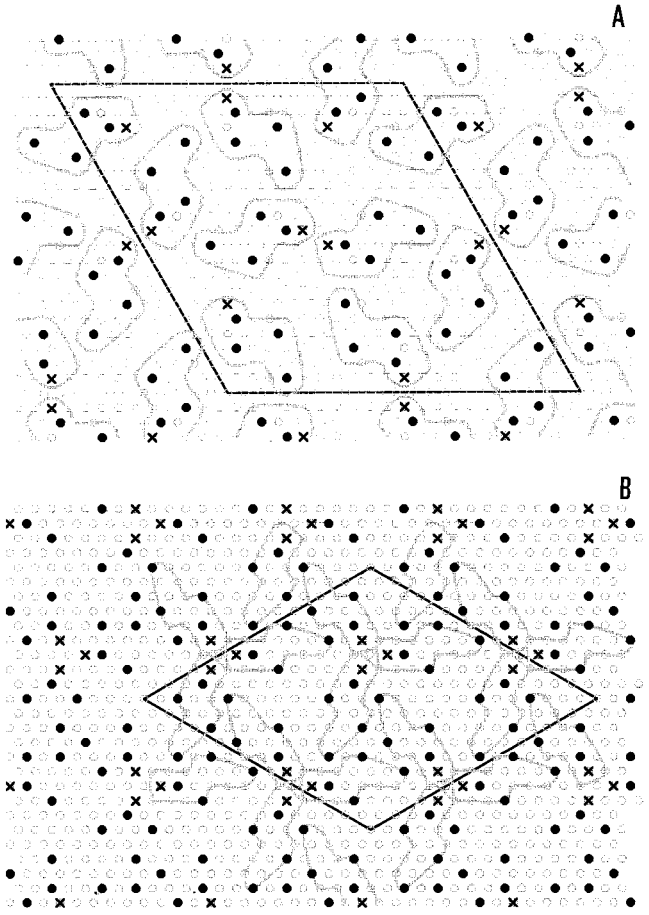

FIGURE 4: Projection of the unit cells of annexin V 2-D crystals with symmetry p6 (A) and symmetry p3 (B) on a portion of the 150 × 150 site triangular lattice used to mimic a lipid layer in the computer-simulated FRAP experiments. The structural data for the distribution of the obstacles and the apparent shape of annexin V molecules (electron density profiles symbolized by the gray line) were obtained from Voges et al. (*12*) for the p6 crystal and from Brisson et al. (*11*) for the p3 crystal. Cell units were fitted to the matrix using a lipid molecular area of 0.63 nm^2. The open symbols represent the obstacle-free sites. The other symbols relate to the obstacles, that is, the four phosphatidylserine molecules (●) which are bound to each annexin V molecule via a calcium bridge and the Trp187 (×) which interacts with the lipid polar headgroups. Note that, in the p6 and p3 crystals, the distribution of the obstacles at the level of each annexin V molecule was the same.

number of obstacles randomly distributed (Table 1). With the p6 crystal and without the central trimer, the four PS molecules and Trp187 provide an obstacle surface concentration S of 7% and a D^*c value of 0.79 which is far above the experimental value of ~0.6. Upon addition of the central trimer, S increased to 10.2% and D^*c decreased to 0.74, a value which is still above the experimental one. It is worth noting that, for the various obstacle configurations examined, D^*c was systematically lower than D^*r, indicating that the lateral motion of lipids is more affected by a regular than by a random distribution of obstacles.

It is clear from the above that a 40% decrease in D ($D^* = 0.6$) requires the presence of additional obstacles. An interesting possibility is to consider the three hydrophobic amino acid residues (Leu31, Ala103, Ala262) which are located on loops AB in close proximity to the PS-binding sites and which, like Trp187, have been suggested to interact with the lipid polar headgroups (*9*, *37*). $D^* = 0.6$ was approximated only for the full p6 crystal with the three additional obstacles ($D^*c \sim 0.61$), a configuration to which a relatively high obstacle area fraction $S = 16.3\%$ corresponds. Other interfacial residues in annexin V have recently been suggested to interact with phospholipid headgroups which could therefore also contribute to a reduction in D (*41*). For the sake of comparison the influence of an obstacle lattice imposed by protein crystals with symmetry p3 was tested as well. As compared to the p6 crystals, the p3 crystals provided a higher obstacle surface density and were therefore more efficient in reducing the lateral motion of lipids. D^*c values of 0.4 or 0.61 were found depending on whether the additional obstacles were considered, suggesting that the p3 crystal is a good candidate to explain the observed decreases in the diffusion coefficient. However, in the electron microscope (*11*, *33*), p3 crystals were detected for protein/lipid complexes adsorbed on grids coated with a continuous carbon film and not when holey grids were used (A. Brisson, personal communication). They were not found by AFM in contact with lipid bilayers (*15*), and it is unlikely that they formed at the much lower protein concentrations ($C_{annexin} <$ 80 nM) used in the present study. Note that other parameters, like changes in the orientation and hydration of the lipid polar headgroups due to interactions with the protein, might also contribute to a slight decrease in D^*. Besides an absence of any quantitative data, this hypothesis could not be tested with the present approach. Altogether and consistent with the AFM data (*15*), the long-range motional behavior of PC molecules in the proteolipid complexes may reasonably be explained using the obstacle configuration imposed by annexin V p6 crystals, provided the central trimer and additional obstacles are taken into account.

To conclude, all of the data described in this work and cited in references was obtained with membrane model systems and the question arises of the significance of these results at the level of biological membranes. It is clear from the available data that annexin V has great potential for forming micro crystals as soon as it reaches the surface of a membrane where acidic lipids are present, more than likely via intermediate trimeric units (*11*, *12*, *15*). In this work, it is clearly shown that micro crystals of annexin V may considerably affect the lateral motion of those acidic lipids to which the protein is firmly attached and in turn the lateral mobility of the other lipids. It is tempting to suggest that, in living cells and at the level of the cytoplasmic leaflet of the plasma membrane where phosphatidylserine molecules are mostly located (*42*), annexin V may form patches of trimeric units capable of sequestering the acidic lipids and of strongly affecting their lateral motion and in turn that of the other lipids and probably of adjacent membrane proteins. This could interfere with those membrane functions which depend on the availability and lateral mobility of these various molecules. In this respect, annexin V has recently been shown to affect the activity of protein kinase C via a mechanism of sequestration of phosphatidylserine molecules (*43*).

ACKNOWLEDGMENT

We wish to thank Drs. A. Brisson, C. Le Grimellec, and V. Vié for fruitful discussions.

REFERENCES

1. Crumpton, M. J., and Dedman, J. R. (1990) *Nature 345*, 212.
2. Creutz, C. E. (1992) *Science 258*, 924−931.

3. Geisow, M. J., Fritsche, U., Hexham, J. M., Dash, B., and Johnson, T. (1986) *Nature 320*, 636−638.
4. Raynal, P., and Pollard, H. B. (1994) *Biochim. Biophys. Acta 1197*, 63−93.
5. Liemann, S., and Lewit-Bentley, A. (1995) *Structure 3*, 233−237.
6. Huber, R., Romisch, J., and Paques, E. P. (1990) *EMBO J. 9*, 3867−3874.
7. Huber, R., Schneider, M., Mayr, I., Romisch, J., and Paques, E. P. (1990) *FEBS Lett. 275*, 15−21.
8. Lewit-Bentley, A., Morera, S., Huber, R., and Bodo, G. (1992) *Eur. J. Biochem. 210*, 73−77.
9. Huber, R., Berendes, R., Burger, A., Schneider, M., Karshikov, A., Luecke, H., Romisch, J., and Paques, E. (1992) *J. Mol. Biol. 223*, 683−704.
10. Concha, N. O., Head, J. F., Kaetzel, M. A., Dedman, J. R., and Seaton, B. A. (1993) *Science 261*, 1321−1324.
11. Brisson, A., Mosser, G., and Huber, R. (1991) *J. Mol. Biol. 220*, 199−203.
12. Voges, D., Berendes, R., Burger, A., Demange, P., Baumeister, W., and Huber, R. (1994) *J. Mol. Biol. 238*, 199−213.
13. Berendes, R., Burger, A., Voges, D., Demange, P., and Huber, R. (1993) *FEBS Lett. 317*, 131−134.
14. Saurel, O., Cézanne, L., Milon, A., Tocanne, J. F., and Demange, P. (1998) *Biochemistry 37*, 1403−1410.
15. Reviakine, I., Bergsma-Schutter, W., and Brisson, A. (1998) *J. Struct. Biol. 121*, 356−361.
16. Rouser, G., Fleischer, S., and Yamamoto, A. (1970) *Lipids 5*, 494−496.
17. Budisa, N., Steipe, B., Demange, P., Eckerskorn, C., Kellermann, J., and Huber, R. (1995) *Eur. J. Biochem. 230*, 788−796.
18. Burger, A., Berendes, R., Voges, D., Huber, R., and Demange, P. (1993) *FEBS Lett. 329*, 25−28.
19. Funakoshi, T., Hendrickson, L. E., Mcmullen, B. A., and Fujikawa, K. (1987) *Biochemistry 26*, 8087−8092.
20. Brian, A. A., and McConnel, H. M. (1984) *Proc. Natl. Acad. Sci. U.S.A. 81*, 6159−6163.
21. Kalb, E., Frey, S., and Tamm, L. K. (1992) *Biochim. Biophys. Acta 1103*, 307−316.
22. Nollert, P., Kiefer, H., and Jähnig, F. (1995) *Biophys. J. 69*, 1447−1455.
23. von Tscharner, V., and McConnell, H. M. (1981) *Biophys. J. 36*, 421−427.
24. Lopez, A., Dupou, L., Altibelli, A., Trotard, J., and Tocanne, J. F. (1988) *Biophys. J. 53*, 963−970.
25. Schram, V., Tocanne, J. F., and Lopez, A. (1994) *Eur. Biophys. J. 23*, 337−348.
26. Salomé, L., Cazeils, J. L., Lopez, A., and Tocanne, J. F. (1998) *Eur. Biophys. J. 27*, 391−402.
27. Nagle, J. F. (1993) *Biophys. J. 64*, 1476−1481.
28. Tait, J. F., Gibson, D., and Fujikawa, K. (1989) *J. Biol. Chem. 264*, 7944−7949.
29. Silvius, J. R. (1990) *Biochemistry 29*, 2930−2938.
30. Gilmanshin, R., Creutz, C. E., and Tamm, L. K. (1994) *Biochemistry 33*, 8225−8232.
31. Hinderliter, A. K., Huang, J., and Feigenson, G. W. (1994) *Biophys. J. 67*, 1906−1911.
32. Meers, P., Daleke, D., Hong, K., and Papahadjopoulos, P. (1991) *Biochemistry 30*, 2903−2908.
33. Olofsson, A., Mallouh, V., and Brisson, A. (1994) *J. Struct. Biol. 113*, 199−205.
34. Meers, P. (1990) *Biochemistry 29*, 3325−3330.
35. Meers, P., and Mealy, T. (1993) *Biochemistry 32*, 5411−5418.
36. Follenius-Wund, A., Piémont, E., Freyssinet, J. M., Gérard, D., and Pigault, C. (1997) *Biochem. Biophys. Res. Commun. 234*, 111−116.
37. Swairjo, M. A., Concha, N. O., Kaetzel, M. A., Dedman, J. R., and Seaton, B. A. (1995) *Nat. Struct. Biol. 2*, 968−974.
38. Seaton, B. A. (1996) in *Annexins: Molecular stucture to cellular function* (Seaton, B. A. Eds.) pp 15−52, Landes, R. G., Company, Heidelberg, Germany.
39. Merkel, R., Sackmann, E., and Evans, E. (1989) *J. Phys. (Paris) 50*, 1535−1555.
40. Berendes, R., Voges, D., Demange, P., Huber, R., and Burger, A. (1993) *Science 262*, 427−430.
41. Campos, B., Mo, Y. D., Mealy, T. R., Li, C. W., Swairjo, M. A., Balch, C., Head, J. F., Retzinger, G., Dedman, J. R., and Seaton, B. A. (1998) *Biochemistry 37*, 8004−8010.
42. Op den Kamp, J. A. F. (1979) *Annu. Rev. Biochem. 48*, 47−71.
43. Dubois, T., Mira, J. P., Defiers, D., Solito, E., Russo-Marie, F., and Oudinet, J. P. (1998) *Biochem. J. 330*, 1277−1282.

BI9818568